Association of cathepsin E with tumor growth arrest through angiogenesis inhibition and enhanced immune responses

Shin, Masashi
Department of Pharmacology, Graduate School of Dental Science, Kyushu University

Kadowaki, Tomoko
Department of Pharmacology, Graduate School of Dental Science, Kyushu University

Iwata, Junichi
Department of Pharmacology, Graduate School of Dental Science, Kyushu University

Kawakubo, Tomoyo
Department of Pharmacology, Graduate School of Dental Science, Kyushu University

他

出版情報：Biological Chemistry. 388 (11), pp.1173-1181, 2007-11-02. De Gruyter
バージョン：

Biol. Chem., Vol. 388, pp. 1173–1181, November 2007 • Copyright © by Walter de Gruyter • Berlin • New York. DOI 10.1515/BC.2007.154

Association of cathepsin E with tumor growth arrest through angiogenesis inhibition and enhanced immune responses

Masashi Shin[1], Tomoko Kadowaki[1], Jun-ichi Iwata[1], Tomoyo Kawakubo[1], Noriko Yamaguchi[2], Ryosuke Takii[1], Takayuki Tsukuba[1,a] and Kenji Yamamoto[1,*]

[1] Department of Pharmacology, Graduate School of Dental Science, Kyushu University, Fukuoka 812-8582, Japan

[2] Department of Cell Biology and Histology, Akita University School of Medicine, Akita 010-8543, Japan

* Corresponding author
e-mail: kyama@dent.kyushu-u.ac.jp

Abstract

Cathepsin E (CE) is an intracellular aspartic proteinase implicated in various physiological and pathological processes, yet its actual roles *in vivo* remain elusive. To assess the physiological significance of CE expression in tumor cells, human CE was stably expressed in human prostate carcinoma ALVA101 cells expressing very little CE activity. Tumor growth in nude mice with xenografted ALVA101/hCE cells was slower than with control ALVA101/mock cells. Angiogenesis antibody array and ELISA assay showed that this was partly due to the increased expression of some antiangiogenic molecules including interleukin 12 and endostatin in tumors induced by CE expression. *In vitro* studies also demonstrated that, among the cathepsins tested, CE most efficiently generated endostatin from the non-collagenous fragment of human collagen XVIII at mild acidic pH. Histological examination revealed that tumors formed by ALVA101/hCE cells were partitioned by well-developed membranous structures and covered with thickened, well-stratified hypodermal tissues. In addition, both the number and extent of activation of tumor-infiltrating macrophages were more profound in ALVA101/hCE compared to ALVA101/mock tumors. The chemotactic response of macrophages to ALVA101/hCE cells was also higher than that to ALVA/mock cells. These results thus indicate that CE expression in tumor cells induces tumor growth arrest via inhibition of angiogenesis and enhanced immune responses.

Keywords: angiogenesis; aspartic proteinase; cathepsin E; endostatin; immune systems; tumor growth.

[a] Present address: Division of Oral Pharmacology, Nagasaki University Graduate School of Biomedical Science, Nagasaki 852-8588, Japan.

Introduction

The growth and metastasis of tumor cells are dependent on their interaction with host defense mechanisms. Therefore, the microenvironment interacting with tumor cells is a promising area for the development of novel tumor therapies. Because angiogenesis is an essential step for tumor progression, antiangiogenic treatments are likely to prevent tumor progression. The discovery of endogenous angiogenic inhibitors such as angiostatin and endostatin has thus led to the realization that proteinases able to generate these antiangiogenic molecules *in vivo* could be considered for therapeutic use. Meanwhile, recent studies have demonstrated that tumor-infiltrating effector cells, including granulocytes, macrophages, natural killer cells, and T- and B-lymphocytes, are critical for antitumor immune responses. Among these cells, macrophages are thought to represent the most important part of the host defense against neoplasm via several mechanisms: killing of neoplastic cells by phagocytosis; antigen processing and presentation to T4 lymphocytes; and enhanced secretion of various cytokines, including TNF-α, interleukin (IL)-1, IL-6 and IL-8, that play crucial roles in non-specific host defense (van Ravenswaay et al., 1992; Naama et al., 2001; Varney et al., 2002). In addition, tumor-associated macrophages were shown to be associated with the induction of tumor cell-specific apoptosis through TNF-related apoptosis ligand (TRAIL)-dependent mechanisms (Griffith et al., 1999; Herbeuval et al., 2003). In the tumor microenvironment, therefore, it is more likely that multiple mechanisms are involved in host defense against neoplasm.

The proteolytic activity of various types of proteases, including lysosomal cathepsins (B, L, and D) and matrix metalloproteinases (MMP-1, MMP-9), have long been associated with many types and stages of cancer (reviewed in Nomura and Katunuma, 2005; Overall and Kleifeld, 2006) and are thought to be attractive cancer targets. However, several strategies designed to broadly block such proteases have been unsuccessful, probably owing to their functional diversity *in vivo*. However, some of the MMP family members, such as MMP-3, MMP-8 and MMP-12, have recently been shown to exhibit beneficial antitumor effects through suppression of tumor angiogenesis and degradation of chemokines that mediate organ-specific metastasis (Overall and Kleifeld, 2006). To establish a new strategy for cancer drug discovery, therefore, it is essential to identify and validate target proteases in various types and stages of cancer. Cathepsin E (CE) is an endolysosomal aspartic proteinase predominantly expressed in cells of the immune system. In antigen-presenting cells (APCs) such as macrophages, microglia, and dendritic cells, CE is found mainly in the endosomal structure as a mature form (Sastradipura et al., 1998; Nishioku et al., 2002), whereas in lymphocytes

such as splenocytes and thymocytes it is mainly localized in the endoplasmic reticulum and Golgi complex as a proform (Sakai et al., 1989; Nishishita et al., 1996; Nishioku et al., 2002). The expression of CE in APCs (Nakanishi et al., 1993; Sastradipura et al., 1998; Tominaga et al., 1998; Yanagawa et al., 2006) and B-cells (Bennett et al., 1992; Sealy et al., 1996) was enhanced by their activation, and a significant amount of the activated enzyme was secreted extracellularly by activated macrophages (Yanagawa et al., 2006). Furthermore, CE was shown to play an important role in the processing of exogenous antigens for the presentation by major histocompatibility complex class II molecules (Bennett et al., 1992; Sealy et al., 1996; Chain et al., 2005). Recent studies with mice deficient in CE also demonstrated that this protein could contribute to the maintenance of homeostasis by participating in host defense mechanisms (Tsukuba et al., 2003, 2006). Subsequent analysis of peritoneal macrophages derived from CE-deficient mice indicated that deficiency in this enzyme induced a novel form of lysosomal storage disorder, manifest as the accumulation of major lysosomal membrane sialoglycoproteins such as LAMP-1 and LAMP-2 and the elevation of lysosomal pH (Yanagawa et al., 2007). However, because physiological substrates of CE have not yet been identified, the relevance of these observations to the physiological functions of this protein remains speculative. Here we show that CE expression in tumor cells is associated with inhibition of angiogenesis and enhanced immune responses, thereby leading to tumor growth arrest.

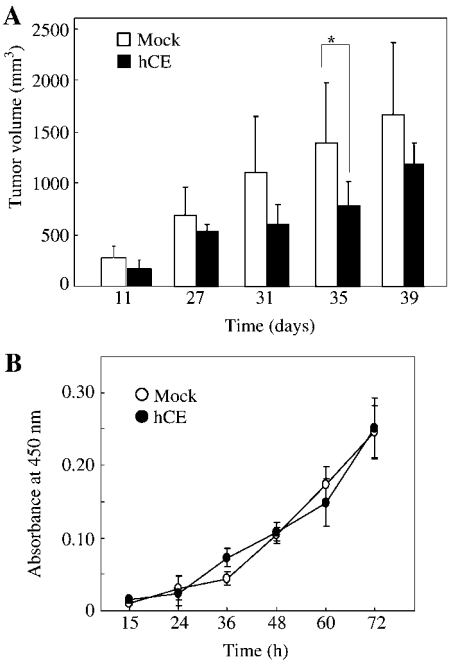

Figure 1 Effect of cathepsin E expression on the *in vivo* (A) and *in vitro* growth (B) of ALVA101 cells.
(A) ALVA101/hCE or ALVA101/mock cells (1×10^7 cells for each) were injected subcutaneously into the flanks of male nude mice. Tumor volumes were calculated using the formula width$^2\times$length$\times$052. Data are mean$\pm$SD of values for six mice per group. *$p<0.05$. (B) ALVA101/hCE or ALVA101/mock cells (5×10^3 cells/well) were seeded into 96-well plates and incubated at 37°C in a CO_2 incubator for the times indicated. Cell proliferation was measured using a Cell Counting Kit 8. Data are the mean$\pm$SD of values for four independent experiments.

Results

Proliferation of ALVA101 cells after human CE and mock transfection

To understand the physiological significance of CE expression in tumor cells, we first generated a stable transfectant of human CE for ALVA101 cells (ALVA101/hCE) and a control transfectant (ALVA101/mock) using the human CE expression vector. CE activity, verified using the specific fluorescent substrate KYS-1 [MOCAc-Gly-Ser-Pro-Ala-Phe-Leu-Ala-Lys(DNP)-D-Arg-NH_2] (Yasuda et al., 2005), was approximately 10-fold higher in ALVA101/hCE compared to ALVA101/mock cells. When each of the transfectants was subcutaneously injected into nude mice, the growth rate of tumors formed by ALVA101/hCE cells was slower than that by ALVA101/mock cells at 39 days post-implantation (Figure 1A). Contrary to the *in vivo* behavior, however, there were no significant differences in the rate of cell proliferation between the two transfectants *in vitro*, indicating the importance of microenvironment interacts for the growth of tumor cells.

CE affects microvessel formation

Several lines of evidence indicate that angiogenesis is essential for the growth and persistence of solid tumors and metastasis (Folman, 1989; Kim et al., 1993; Millauer et al., 1994), indicating that tumor growth is regulated by a balance between positive and negative factors for angiogenesis. To assess the mechanism by which the tumor growth in nude mice bearing ALVA101/hCE cells was lower than in those bearing ALVA101/mock cells, we examined the expression levels of multiple angiogenic factors in each of the tumor lysates using an angiogenesis antibody array. The expression levels of IL-12 p40/p70 and monokine induced by γ-interferon (MIG) were significantly increased in tumor lysates from nude mice bearing ALVA101/hCE cells compared to those with ALVA101/mock cells, whereas levels of tissue inhibitor of metalloproteinases (TIMP)-1 and platelet factor (PF) were decreased by CE transfection (Figure 2). It has been shown that while IL-12 and MIG act as antitumor molecules, TIMP-1 has the ability to promote cell proliferation and to inhibit the proteolytic activity of metalloproteinase family members. PF-4 has been shown to inhibit endothelial proliferation and angiogenesis. The contradictory data on PF-4 may be explained by the pleiotropic nature and ill-defined functions of this molecule. We further determined expression levels of endostatin in sera and tumor lysates from nude mice subcutaneously implanted with each of the transfectants using an endostatin ELISA kit. Endostatin is a potent endogenous antiangiogenic protein with an apparent molecular mass of 22 kDa that is capable of inhibiting endothelial cell proliferation (O'Reilly et al., 1996, 1997) and migration (Yamaguchi et al., 1999), and is proteolytically generated from the C-terminal non-collagenous (NC1) fragment of collagen XVIII (Felbor et al., 2000; Ferreras et al., 2000). Endostatin levels in both the serum and tumor lysate from mice implanted with ALVA101/hCE cells were higher than

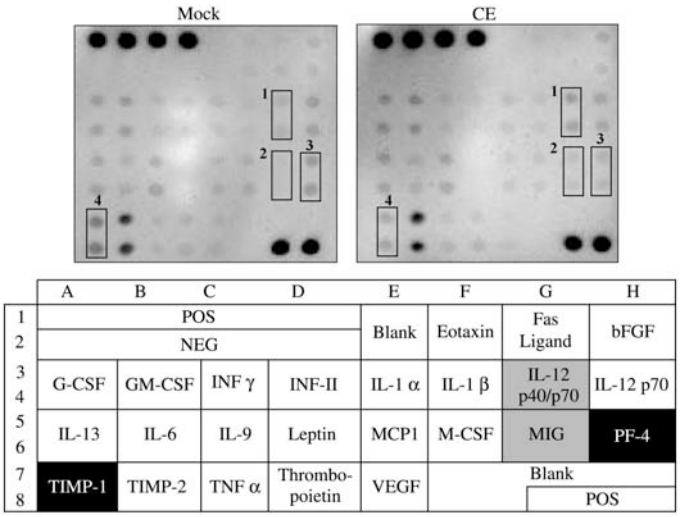

Figure 2 Angiogenesis antibody array for lysates from tumors formed by ALVA101/hCE and ALVA101/mock cells. Tumors extirpated from nude mice 64 days post-implantation were homogenized and lysed. Samples of 500 μg of protein extracts were used for the antibody array. Numbered rectangles: 1, IL-12 p40/p70; 2, MIG; 3, PF-4; and 4, TIMP-1.

those treated with ALVA101/mock cells (Figure 3). The results thus indicate that the growth of tumors formed by ALVA101/hCE cells was suppressed, at least in part, by an increase in antiangiogenesis molecules and a decrease in angiogenesis molecules.

Characterization of endostatin generation from the NC1 domain of collagen XVIII by CE and other cathepsins *in vitro*

To understand the process of endostatin generation by CE, we tested its ability to generate endostatic fragments from the NC1 fragment of collagen XVIII at pH 6.0 and compared its efficiency with that of other cathepsins (D, B, L, and H) purified from rat sources as previously described (Yasuda et al., 2005). Each purified enzyme was incubated at 37°C for 12 h with recombinant NC1 at the same molar ratio (NC1/enzyme 7.2:1). The reaction products were then analyzed by SDS-PAGE and immunoblotting with polyclonal antibodies to recombinant human endostatin. As shown in Figure 4A, CE most effectively converted NC1 into a 22-kDa endostatin-like fragment. Although CD and CL also cleaved NC1 to generate endostatin-like fragments, their efficiency (in terms of the extent and stability of the products) was much less than that of CE. Both CB and CH exhibited little or no activity to generate endostatin-like fragments from NC1. At pH 5–6, CE most efficiently generated the 22-kDa endostatin-like fragment; however, this fragment was degraded further by CE at pH 4 (data not shown). Generation of the 22-kDa endostatin-like fragment by CE was also found to be dose- and time-dependent (data not shown). The N-terminal amino acid sequence of the 22-kDa fragment generated by CE and CD was found to be VHLRPAPT, which corresponds to the sequence of human collagen XVIII beginning at Val^{118} (Figure 4B) and is identical to that found in human tissues and plasma (Standker et al., 1997; Sasaki et al., 1998). Differing from CE, however, CD cleaves at an additional site beginning at Leu^{71}. On the other hand, the previously defined sequence of mouse endostatin generated by CL begins at His^{131} (Felbor et al., 2000). Besides CL, CB and CK were previously shown to process the NC1 domain to an endostatic fragment with an N-terminus beginning at Leu^{120} (Ferreras et al., 2000). Matrix metalloproteinases including MMP-3, -9, -12, -13, and -20 can also process human NC1 to generate endostatin-like fragments with N-termini beginning at Tyr^{108} and Ser^{115} (Standker et al., 1997). However, it should be noted that endostatin-like molecules with an N-terminus identical to those generated by any of these proteinases, except for CE and CD, have not been detected in human tissues and plasma. Given the most efficient generation of endostatin by CE under moderately acidic conditions similar to the microenvironment of tumors, this enzyme seems the most likely candidate responsible for endostatin generation *in vivo*.

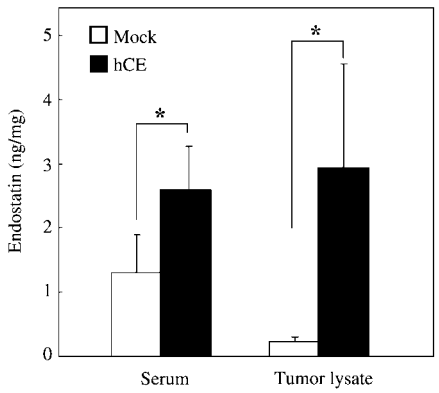

Figure 3 Endostatin levels in serum and tumor lysates from nude mice implanted with ALVA101/hCE or ALVA101/mock cells. Tumors extirpated from nude mice 30 days post-implantation were homogenized in lysis buffer. Endostatin levels in serum and tumor lysates were measured by ELISA. Data are the mean±SD of values for four mice per group. *$p<0.05$.

Effect of CE on tube formation and destruction by HUVECs

We further examined whether the efficiency of endostatin generation by each cathepsin was correlated to the

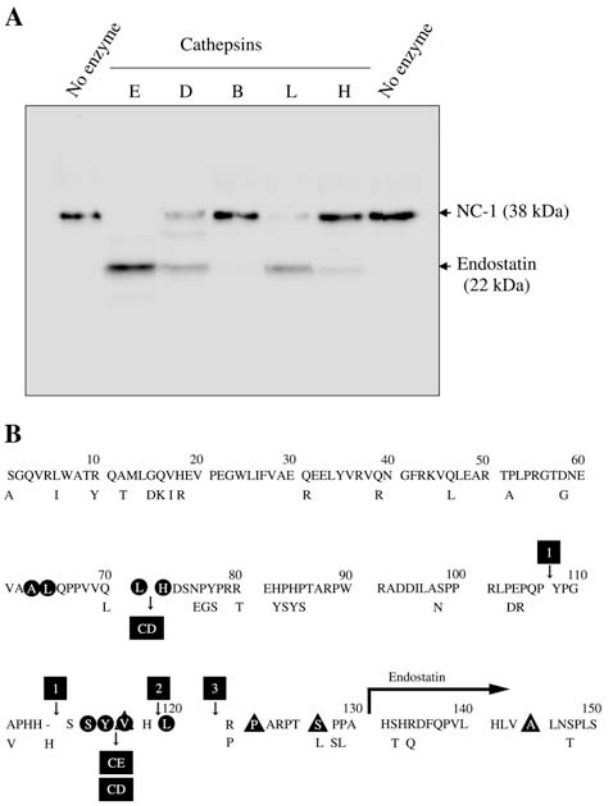

Figure 4 Processing of the NC1 domain of collagen XVIII by purified cathepsins.
(A) Recombinant NC1 (0.275 μg) was incubated with various cathepsins (CE, CD, CB, CL, and CH) at concentrations of 1×10^{-12} mol in pH 6.0 buffer at 37°C for 13 h. Each sample was then analyzed by SDS-PAGE and immunoblotting using an anti-endostatin antibody. (B) Cleavage sites of the NC1 domain by CE and CD compared to those by other proteinases. Data for the amino acid sequence of human collagen XVIII and its substitutions in mouse collagen XVIII indicated below are from Oh et al. (1994a,b). The NH_2-terminal sequences of endostatin-like fragments detected in human and mouse plasma are shown by full circles and full triangles, respectively. Numbers 1, 2, and 3 in black boxes indicate cleavage sites by MMP-9 (no. 1), CL (no. 2), CB (no. 2), CK (no. 2), and pancreatic elastase (no. 3) reported by Felbor et al. (2000) and Ferreras et al. (2000). The thick arrow indicates the NH_2-terminal sequence of the originally described mouse endostatin.

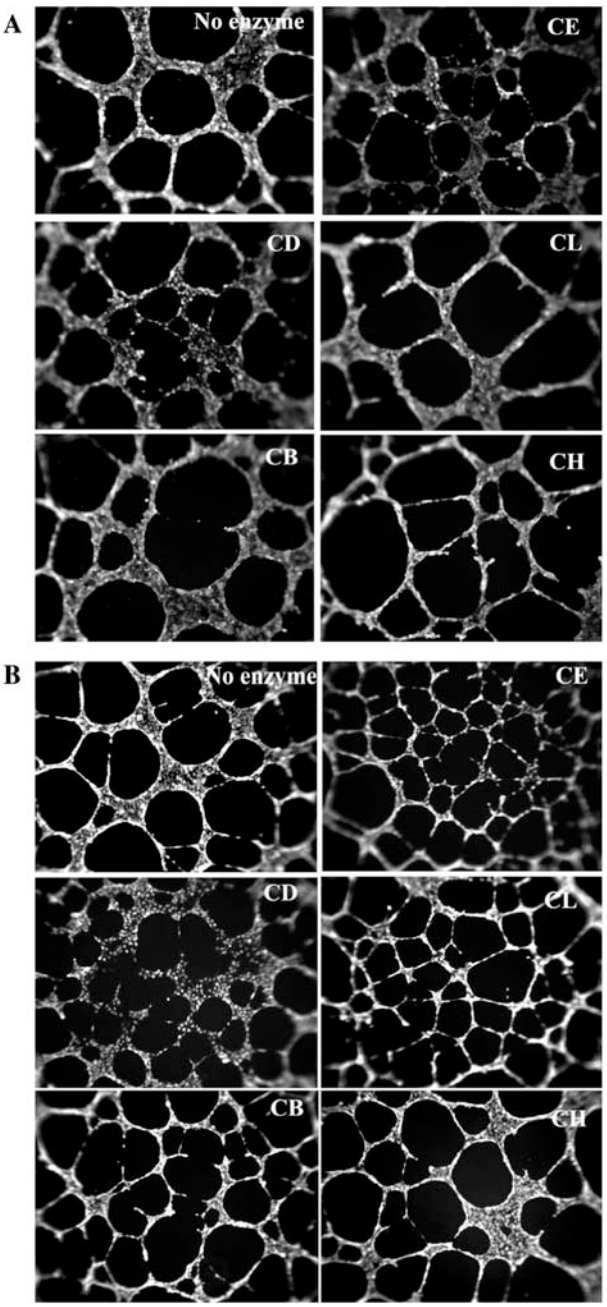

Figure 5 Effects of various cathepsins on tube formation (A) and tube destruction (B) of HUVECs.
(A) HUVECs (1×10^4 cells/well) were cultured with recombinant NC1 (0.275 μg) and each purified cathepsin (5×10^{-12} mol) on Matrigel in 96-well tissue culture plates for 18 h. Viable cells were then labeled with Calcein AM (1 μM) and observed by fluorescence microscopy. Individual experiments were performed in at least triplicate and representative images from four independent experiments are shown. (B) HUVECs (1×10^4 cell/well) were cultured on Matrigel for 7 h. Then recombinant NC1 (0.55 μg) and each cathepsin (5×10^{-12} mol) were added to the culture and incubated for an additional 13 h. Photomicrographs were obtained as for (A).

extent of inhibition of endothelial tube formation by a Matrigel tube formation assay, which is known to represent various aspects of angiogenesis including cellular migration and differentiation (Grant et al., 1991). Human umbilical vein endothelial cells (HUVECs) were cultured on Matrigels in the presence of NC1 with or without each cathepsin. Consistent with the efficiency of endostatin generation, CE, as well as CD, was found to most efficiently inhibit tube formation, whereas CL, CB, and CH exhibited little effect on this process (Figure 5). Although the efficiency of endostatin generation from NC1 by CD was relatively less than that by CE (Figure 4), no significant differences in the extent of inhibition of tube formation were observed between the two enzymes, suggesting the presence of additional mechanisms for inhibition of tube formation by CD. Given the ability of endostatin to induce apoptosis of endothelial cells (O'Reilly et al., 1997; Dhanabal et al., 1999a,b), besides its potential to inhibit tube formation, we further examined whether the efficiency of endostatin generation was correlated to the extent of endothelial tube destruction by cathepsins. The extent of the destruction of endothelial tubes that had been formed on Matrigels also appeared to be correlated to the efficiency of endostatin

generation (Figure 5B). CE and CD, but not CL, CB and CH, efficiently destroyed the tubes and dispersed the endothelial cells.

Morphological observation of tumors formed by ALVA101/hCE and ALVA101/mock cells

As shown in Figure 6A, the tumors formed by ALVA101/hCE cells at 29 days post-inoculation showed more polymorphous and irregular margins and were covered by a more thickened skin compared with those formed by ALVA101/mock cells at the same age. At a microscopic level, the tumors formed by ALVA101/hCE cells were found to be partitioned by well-developed membranous structures and covered with thick, well-stratified dermal tissues, while those for ALVA101/mock cells exhibited a large solid mass surrounded by thin membrane structures (Figure 6B). Strikingly, at higher magnification, the tumors formed by ALVA101/hCE cells were bordered by thick, well-stratified dermal and mesenchymal tissues (Figure 6C). The thickened hypodermal tissues adjacent to the tumors formed by ALVA101/hCE cells were characterized by progressive and diffuse hyperplasia of fibrous membranes, fat tissue, and sebaceous gland-like structures. These results suggest that CE expression in tumor cells may direct them to normal cell proliferation and differentiation.

Strikingly, further immunohistochemical studies showed a large number of tumor-infiltrating effector cells, including lymphocytes and macrophages, both within and nearby the tumors formed by each of the transfectants. However, both the number and the extent of activation of tumor-infiltrating macrophages close to the tumors were greater in ALVA101/hCE compared to ALVA101/mock xenografts, as revealed by immunostaining with antibodies to the F4/80 antigen (Figure 6D, lower panels). In contrast, the number of CD3-positive T-lymphocytes within tumors was greater in ALVA101/mock compared to ALVA101/hCE xenografts (Figure 6D, upper panels). Although the vascularity within tumors was not significantly different between the two xenografts, the integrity of vascular endothelial cells in this area appeared to be vitiated in ALVA101/mock compared to ALVA101/hCE xenografts (data not shown). Therefore, the difference in the density of CD3-positive T-lymphocytes is probably due to the difference in vascular integrity between the two xenografts.

Chemotactic responses of macrophages to ALVA101/hCE and ALVA101/mock cells

To assess the effect of CE expression in tumor cells, the chemotactic response of macrophages to ALVA101/hCE and ALVA101/mock cells was analyzed using a Boyden chamber system in the presence or absence of monocyte chemoattractant protein (MCP)-1. The chemotactic response of macrophages was much higher (1.6-fold) to ALVA101/hCE than to ALVA101/mock cells in the absence of MCP-1 (Figure 7). The higher chemotactic response of macrophages to ALVA101/hCE cells was still retained in the presence of MCP-1. Given that MCP-1 protein levels in cell extracts of tumors formed by ALVA101/hCE cells tended to be lower than in those formed by ALVA101/mock cells (7.43±2.99 pg/mg protein vs. 13.49±3.97 pg/mg protein), additional factors other than MCP-1 are likely to be involved in enhancement of the chemotactic response of macrophages by CE expression.

Discussion

In this study, we provide the first evidence that CE expression in tumor cells is associated with growth arrest *in vivo* through the inhibition of tumor-induced angiogenesis and enhanced immune responses. Since the microenvironment interacting with tumor cells and the expression levels of CE in cells were thought to be critical for the regulation of tumor growth, we first examined the effect of CE expression in ALVA101 cells on tumor-induced angiogenesis. ALVA101 is a cell line established from bone metastases of human prostate carcinoma cells (van Bokhoven et al., 2003) and exhibits very little CE activity. Angiogenesis antibody arrays and ELISAs showed that the expression levels of antiangiogenic molecules such as IL-12, MIG, and endostatin were significantly higher in ALVA101/hCE compared to ALVA101/mock xenografts; inversely, levels of cell proliferation molecules such as TIMP were lower in ALVA101/hCE compared to ALVA101/mock xenografts. *In vitro* studies also demonstrated that purified CE had a strong ability to generate a 22-kDa endostatic fragment from recombinant NC1 by specific cleavage of the Tyr^{117}-Val^{118} bond. This fragment was 13 residues longer at the N-terminus than the original mouse endostatin, but was identical to that found in human tissues and plasma. Endostatin generation by CE was the most potent compared to other cathepsins. Consistent with this, the efficiency of endostatin generation by serum-free culture medium from ALVA101/hCE cells was greater than for ALVA101/mock cells (data not shown), indicating a direct correlation between CE expression levels and the efficiency of endostatin generation. Furthermore, the endostatic fragment generated by CE was shown to have the potential to induce both tube formation and destruction on Matrigels using HUVECs. Our data also indicate that production of the endostatin fragment by CE is most efficient under moderately acidic conditions such as pH 6.0. Given that tumor cells *in vivo* are exposed to ischemic and hypoxic conditions (Wike-Hooley et al., 1984; Tannock and Rotin, 1989) and that a proton gradient contributing to the synthesis of ATP at the cell surface is detected in the extracellular milieu of tumors (Gerweck et al., 1991), the center of tumors is likely more acidic than the surface or regions near blood vessels. Therefore, the mild acidic microenvironment of primary tumor sites might provide the most suitable conditions for endostatin generation by CE.

In this study, we also demonstrated for the first time that CE expression by tumor cells enhanced host immune responses. The extent of tumor-infiltrated effector cells, particularly activated macrophages, in the vicinity of the subcutaneous inoculation site was greater in ALVA101/hCE compared to ALVA101/mock xenografts. Given the ability of tumor-infiltrating macrophages to

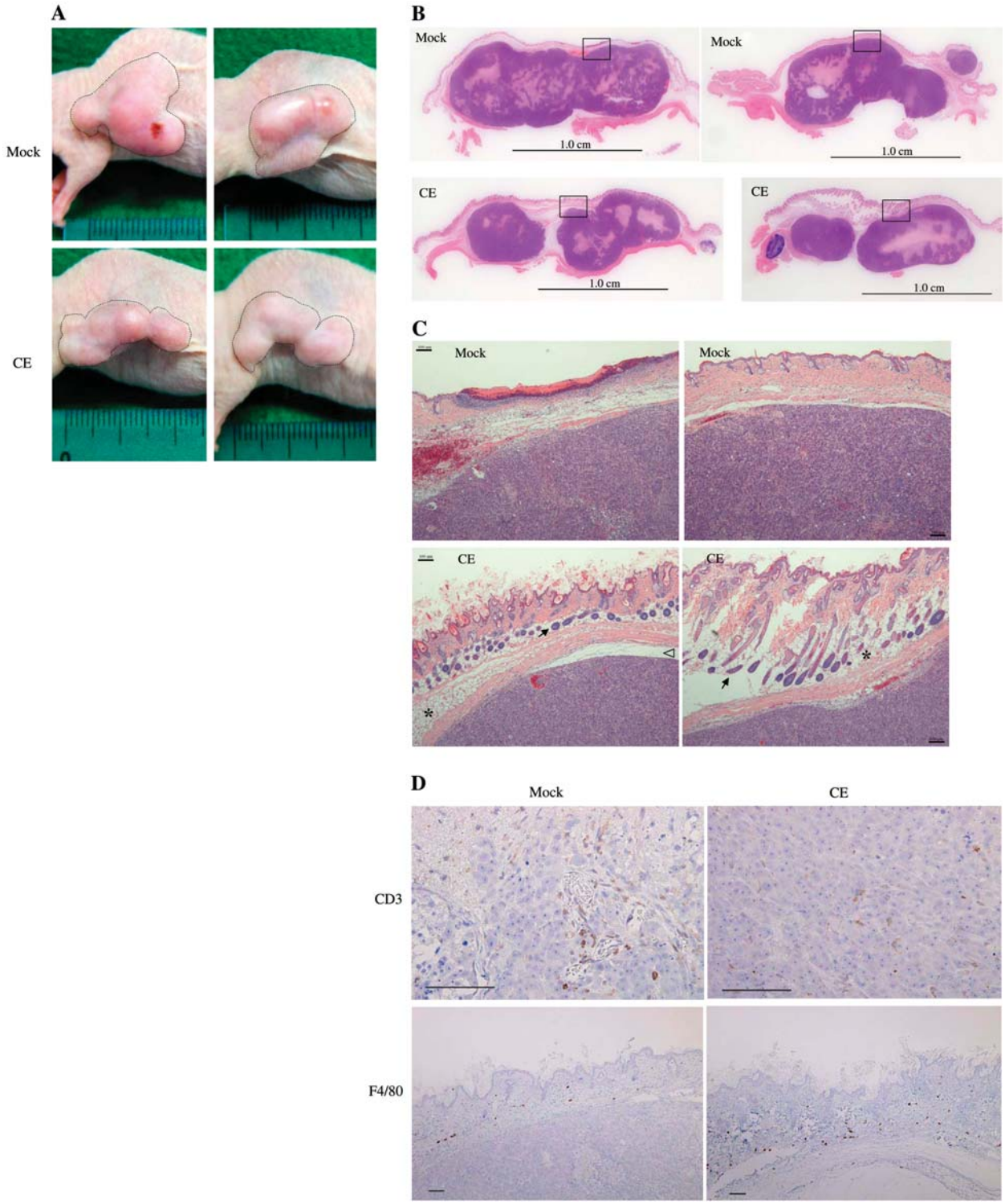

Figure 6 Morphological observations of xenografts from nude mice implanted with ALVA101/hCE and ALVA101/mock cells. (A) Gross appearances of nude mice bearing ALVA101/hCE and ALVA101/mock cells at 29 days post-implantation. (B) Histological observation of HE-stained samples. The xenografts formed by ALVA101/hCE cells at 29 days post-inoculation showed more polymorphous and irregular margins and were covered by more thickened skin compared to those formed by ALVA101/mock cells at the same age. (C) Enlargement of the square regions of each xenograft in (B). The thickened hypodermal tissues adjacent to the tumors formed by ALVA101/hCE cells were characterized by progressive and diffuse hyperplasia of fibrous membranes (open arrowhead), fat tissue (asterisks), and sebaceous gland-like structures (arrows). A representative micrograph from four animals is shown for each group. Scale bars represent 100 μm. (D) Immunohistochemical staining of tumors from nude mice bearing ALVA101/hCE and ALVA101/mock cells at 29 days post-implantation with antibodies against the F4/80 antigen and CD3. After treatment with biotinylated secondary antibody and streptavidin HRP reagent, the sections were reacted with 3,3′-diaminobenzidine and counterstained with HE. Scale bars represent 100 μm.

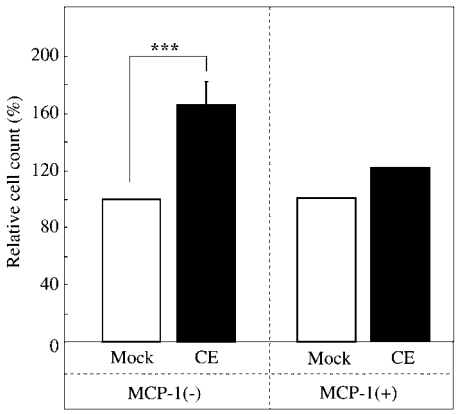

Figure 7 Chemotactic response of macrophages toward ALVA101/hCE and ALVA101/mock cells.
ALVA101/hCE or ALVA101/mock cells were seeded into the bottom wells of cell migration chambers, and mouse peritoneal macrophages were added to inserts with a pore size of 8 μm and placed into each culture well. After incubation for 2 h at 37°C in the absence or presence of MCP-1, the membrane filters were washed, fixed and stained with May-Giemsa stain before counting under a light microscope. Data are the mean±SD of values from five independent experiments. ***$p<0.001$.

attack and eliminate tumor cells through contact-dependent and cytokine-mediated mechanisms (Holen et al., 2002), it is reasonable to infer that tumor-infiltrated macrophages, together with other cell types of the immune system, function to inhibit tumor growth and metastasis. Our data demonstrate that both the number and the extent of activation of tumor-infiltrated macrophages were apparently increased in ALVA101/hCE compared to ALVA101/mock xenografts. Therefore, CE expression levels in tumor cells appear to be strongly associated with a decrease in tumor growth through the enhanced infiltration and activation of tumor-associated macrophages. In this regard, our data also show that the chemotactic response of macrophages was greater in ALVA101/hCE compared to ALVA101/mock cells. Although it still remains to be established how CE expression in tumor cells induces the enhanced chemotactic response of macrophages and the increased infiltration and activation of these cells, the present results provide new insight into the functional diversity of CE in host defense against tumor cells. Meanwhile, tumor-promoting effects of tumor-associated macrophages have recently been recognized, such as enhancement of tumor cell migration and invasion, facilitation of extracellular matrix breakdown and remodeling or promotion of tumor cell motility, and stimulation of angiogenesis (Strand et al., 2004). These competing functions of macrophages appear to arise from the pleiotropic nature of these cells, probably due to the production of a variety of cytokines and reactive oxygen species. The present results thus indicate that the stable expression of CE in tumor cells may confer optimal conditions for tumor regression by tumor-infiltrated macrophages. To the best of our knowledge, the proteolytic activity of various types of proteases generated by tumor cells, including CB, CL, CD, MMP-1, and MMP-9, creates a microenvironment favorable for tumor growth and progression (Nomura and Katsunuma, 2005; Overall and Kleifeld, 2006), but limited information is available about proteases that induce tumor growth arrest and inhibition of metastasis. In this regard, CE may represent a novel example of beneficial proteases produced by tumor cells.

Materials and methods

Cells culture

The human prostate cancer cell line ALVA101 was kindly provided by J.Y. Bahk (Gyeogsang National University, Korea) and maintained in Dulbecco's modified Eagle's medium (DMEM) supplemented with 0.1% $NaHCO_3$, 10% fetal bovine serum (Biomedicals, Costa Mesa, CA, USA), penicillin (100 U/ml), streptomycin (100 μg/ml), and 2 mM L-glutamine. HUVECs were maintained in endothelial basal medium (Toyobo, Osaka, Japan).

Stable transfectant of CE

Human CE cDNA was obtained by digestion of pAGS412 (Azuma et al., 1989) with EcoRV and SmaI. The DNA fragment including human CE cDNA was introduced at the EcoRV site of pcDNA3.1 (+). ALVA101 cells were seeded in 100-mm plates, cultured for 24 h, and transfected with 15 μg of hCE/pcDNA3.1 (+) expression vector using 45 μl of TransFast™ transfection reagent (Promega, Madison, WI, USA). As a negative control, the pcDNA3.1 (+) empty vector was introduced into ALVA101 cells. Transfections were carried out according to the manufacturer's instructions. At 48 h post-transfection, the medium was changed to complete culture medium containing 500 μg/ml G418. After 2 weeks of incubation in this medium, G418-resistant colonies were picked out and cloned.

Measurement of CE activity

CE activity was measured according to the method described previously (Yasuda et al., 2005). Briefly, reaction mixtures contained 10 μl of buffer (1 M sodium acetate buffer, pH 3.5), 10 μl of 200 μM KYS-1 fluorogenic substrate (Peptide Institute Inc., Osaka, Japan), and 80 μl of sample solution in a total volume of 100 μl. Reaction mixtures were incubated at 40°C for 10 min and the reaction was terminated by adding 2 ml of 5% trichloroacetic acid. The increase in fluorescence intensity during incubation was measured at an emission wavelength of 393 nm with excitation at 328 nm using a fluorescence spectrophotometer (F-3010; Hitachi, Tokyo, Japan).

Cell proliferation assay

Proliferation of tumor cells was measured using a Cell Counting Kit 8 (Dojin, Kumamoto, Japan). ALVA101/hCE or ALVA101/mock cells (5×10^3 cells for each) were seeded into 96-well plates and incubated at 37°C in a CO_2 incubator for up to 72 h. At the end of this incubation period, sodium 2-(4-Iodophenyl)-3-(4-nitrophenyl)-5-(2,4-disulfophenyl)-2*H*-tetrazolium was added to the culture medium and incubated for an additional 1 h at 37°C. The amount of reduced tetrazolium was determined by measuring the absorbance at 450 nm in a microplate reader (ImunoMini NJ-2300; Nalge Nunc International, Tokyo, Japan).

Implantation of tumor cells

Male athymic nude BALB/c mice were obtained from CLEA Japan Inc. (Osaka, Japan). ALVA101/hCE or mock cells (1×10^7 cells) in phosphate-buffered saline (PBS) were injected subcutaneously into the flank of the nude mice. Tumor size was assessed using calipers every other day. Tumor volume was cal-

culated using the formula width^2×length×0.52. After 4–9 weeks, the mice were sacrificed and the tumors were extirpated. Animals were maintained under specific pathogen-free conditions according to the guidelines of the Japanese Pharmacological Society. All experiments using animals and recombinant DNA in this study were approved by the Animal and Microbiological Research Committee of Kyushu University.

Angiogenesis antibody array

The RayBio™ mouse angiogenesis antibody array was obtained from RayBiotech, Inc. (Norcross, GA, USA). Tumors extirpated at 64 days post-implantation were homogenized and lysed in cell lysis buffer according to the manufacturer's protocol. Samples of 500 μg of protein extracts were used for angiogenesis antibody array analysis.

Quantitative analysis of endostatin

The endostatin ELISA kit was obtained from Cytimmune Sciences (Rockville, MD, USA). Tumors extirpated at 30 days post-implantation were homogenized in lysis buffer consisting of PBS and 0.1% Triton X-100. The tumor lysate was centrifuged at 27 000 *g* for 30 min to remove insoluble particles. Both the lysate and the serum were assayed for endostatin.

In vitro degradation of NC1 by cathepsins

Recombinant NC1 (0.275 μg) was incubated with cathepsins E, D, B, L, and H (1×10^{-12} mol) in pH 6.0 buffer at 37°C for 13 h. For incubation with CB, CL, and CH, dithiothreitol (10 mM) and EDTA (1 mM) were added to the reaction mixture. After incubation, samples were separated by SDS-PAGE, transferred onto nitrocellulose membranes, and subjected to Western blot analysis using an anti-endostatin antibody (Cytimmune Sciences).

Tube formation and destruction assays

Tissue culture plates (96-well) were coated with Matrigel (50 μl/well) (Becton Dickinson, Franklin Lakes, NJ, USA) at 37°C for 30 min, followed by seeding of HUVECs (1×10^4 cell/well). Recombinant NC1 (0.275 μg/well) and CE, CD, CB, CL, or CH (5×10^{-12} mol/well) were added with HUVECs for tube formation assays. The cell cultures were incubated for 18 h. For tube destruction assays, NC1 and each cathepsin were added into wells at 7 h after seeding of HUVECs onto the gels, and then incubated for an additional 13 h. Viable cells were then fluorescent-stained with Calcein AM (1 μM; Molecular Probes, Inc., Eugene, OR, USA), and photographed under fluorescence microscopic observation. Individual experiments were performed in at least triplicate and representative photographs are shown.

Histochemistry and immunohistochemistry

At 29 days post-implantation, tumors were extirpated, fixed with 10% formalin, and embedded in paraffin. Sections were stained with hematoxylin and eosin (HE). Formalin-fixed and paraffin-embedded xenograft sections were further examined by immunohistochemistry for F4/80 and CD3, essentially according to the method described by Sastradipura et al. (1998).

Preparation of peritoneal macrophages

Thioglycolate-elicited peritoneal macrophages were isolated from mice as previously described (Nishioku et al., 2002). Briefly, 8–14-week-old mice were injected peritoneally with 4.05% thioglycolate (2 ml/mouse). At 3.5 days later, peritoneal exudate cells were isolated from the peritoneal cavity by washing with PBS. The cells were incubated with RPMI 1640 medium supplemented with 10% fetal bovine serum, penicillin (50 U/ml), and streptomycin (50 μg/ml) at 37°C with 5% CO_2. After incubation for 2 h, non-adherent cells were removed by washing with Ca^{2+}/Mg^{2+}-free PBS three times. Peritoneal macrophages isolated as adherent MAC-2-positive cells were obtained at a purity of >95%.

Macrophage chemotaxis assay

ALVA101/hCE or ALVA101/mock cells were seeded onto the bottom wells of cell migration chambers (Becton Dickinson). Peritoneal macrophages were added onto filter well inserts (8-μm pore size; Becton Dickinson) and placed into each culture well. Cell migration was assessed by incubation for 2 h in a cell culture incubator at 37°C with 5% CO_2. Cells on the top of the filter were wiped off, and the filter was fixed in methanol and stained with HE. The total number of cells that migrated to the lower side of the filter was determined by averaging the number of cells counted in five random microscope fields (magnification 200×).

Statistical analysis

The statistical significance of differences between experimental and control groups was determined by the two-tailed Student *t*-test. A *p*-value of <0.05 was considered statistically significant.

References

Azuma, T., Pals, G., Mohandas, T.K., Couvreur, J.M., and Taggart, R.T. (1989). Human gastric cathepsin E. Predicted sequence, localization to chromosome 1, and sequence homology with other aspartic proteinases. J. Biol. Chem. *264*, 16748–16753.

Bennett, K., Levine T., Ellis, J.S., Peanasky, R.J., Samloff, I.M., Kay, J., and Chain, B.M. (1992). Antigen processing for presentation by class II major histocompatibility complex requires cleavage by cathepsin E. Eur. J. Immunol. *22*, 1519–1524.

Chain, B.M., Free, P., Medd, P., Swetman, C., Tabor, A.B., and Terrazzini, N. (2005). The expression and function of cathepsin E in dendritic cells. J. Immunol. *174*, 1791–1800.

Dhanabal, M., Ramachandran, R., Volk, R., Stillman, I.E., Lombardo, M., Iruela-Arispe, M.L., Simons, M., and Sukhatme, V.P. (1999a). Endostatin: yeast production, mutants, and antitumor effect in renal cell carcinoma. Cancer Res. *59*, 189–197.

Dhanabal, M., Ramchandran, R., Waterman, M.J.F., Lu, H., Knebelmann, B., Segal, M., and Sukhatme, V.P. (1999b). Endostatin induces endothelial cell apoptosis. J. Biol. Chem. *274*, 11721–11726.

Felbor, U., Dreier, L., Bryant, R.A.R., Ploegh, H.L., Olsen, B.R., and Mothes, W. (2000). Secreted cathepsin L generates endostatin from collagen XVIII. EMBO J. *19*, 1187–1194.

Ferreras, M., Felbor, U., Lenhard, T., Olsen, B.R., and Delaisse, J. (2000). Generation and degradation of human endostatin proteins by various proteinases. FEBS Lett. *486*, 247–251.

Folman, J. (1989). What is the evidence that tumors are angiogenesis dependent? J. Natl. Cancer Inst. *82*, 4–6.

Gerweck, L.E., Rhee, J.G., Koutcher, J.A., Song, C.W., and Urato, M. (1991). Regulation of pH in murine tumor and muscle. Radiat. Res. *126*, 206–209.

Grant, D.S., Lelkes, P.I., Fukuda, K., and Kleinman, H.K. (1991). Intracellular mechanisms involved in basement membrane induced blood vessel differentiation *in vitro*. In Vitro Cell. Dev. Biol. *27A*, 327–336.

Griffith, T.S., Wiley, S.R., Kubin, M.Z., Sedger, L.M., Maliszewski, C.R., and Fanger, N.A. (1999). Monocyte-mediated tumoricidal activity via the tumor necrosis factor-related cytokine, TRAIL. J. Exp. Med. *189*, 1343–1353.

Herbeuval, J.-P., Lambert, C., Sabido, O., Cottier, M., Fournel, P., Dy, M., and Genin, C. (2003). Macrophages from cancer patients: analysis of TRAIL, TRAIL receptors, and colon tumor cell apoptosis. J. Natl. Cancer Inst. *95*, 611–621.

Holen, I., Croucher, P.I., Hamdy, F.C., and Eaton, C.L. (2002). Osteoprotegerin (OPG) is a survival factor for human prostate cancer cells. Cancer Res. *62*, 1619–1623.

Kim, K.J., Li, B., Winer, J., Armanini, M., Gillett, N., Phillips, H.S., and Ferrara, M. (1993). Inhibition of vascular endothelial growth factor-induced angiogenesis suppresses tumor growth *in vivo*. Nature *362*, 841–844.

Millauer, B., Shawver, L.K., Plate, K.H., Risau, W., and Ullrich, A. (1994). Glioblastoma growth inhibited *in vivo* by a dominant-negative Flk-1 mutant. Nature *367*, 576–579.

Naama, H.A., Mack, V.E., Smyth, G.P., Stapleton, P.P., and Daly, J.M. (2001). Macrophage effector mechanisms in melanoma in an experimental study. Arch. Surg. *136*, 804–809.

Nakanishi, H., Tsukuba, T., Kondou, T., Tanaka, T., and Yamamoto, K. (1993). Transient forebrain ischemia induces increased expression and specific localization of cathepsins E and D in rat hippocampus and neostriatum. Exp. Neurol. *121*, 215–223.

Nishioku, T., Hashimoto, K., Yamashita, K., Liou, S.Y., Kagamiishi, Y., Maegawa, H., Katsube, N., Peters, C., von Figura, K., Saftig, P., et al. (2002). Involvement of cathepsin E in exogenous antigen processing in primary cultured murine microglia. J. Biol. Chem. *277*, 4816–4822.

Nishishita, K., Sakai, H., Sakai, E., Kato, Y., and Yamamoto, K. (1996). Age-related and dexamethasone-induced changes in cathepsins E and D in rat thymic and spleen cells. Arch. Biochem. Biophys. *333*, 349–358.

Nomura, T. and Katsunuma, N. (2005). Involvement of cathepsins in the invasion, metastasis and proliferation of cancer. J. Med. Invest. *52*, 1–9.

Oh, S.P., Kamagata, Y., Muragaki, Y., Timmons, S., Ooshima, A., and Olsen, B.R. (1994a). Isolation and sequencing of cDNA for proteins with multiple domains of Gly-Xaa-Yaa repeats identify a distinct family of collagenous proteins. Proc. Natl. Acad. Sci. USA *91*, 4229–4233.

Oh, S.P., Warman, M.L., Seldin, M.F., Cheng, S.D., Knoll, J.H.M., Timmons, S., and Olsen, B.R. (1994b). Cloning of cDNA and genomic DNA encoding human type XVIII collagen and localization of the α1 (XVIII) collagen gene to mouse chromosome 10 and human chromosome 21. Genomics *19*, 494–499.

O'Reilly, M.S., Boehm, T., Shing, Y., Fukai, N., Vasios, G., Lane, W.S., Flynn, E., Birkhead, J.R., Olsen, B.R., and Folkman, J. (1997). Endostatin: an endogenous inhibitor of angiogenesis and tumor growth. Cell *88*, 277–285.

O'Reilly, M.S., Holmgren, L., Chen, C.C., and Folkman, J. (1996). Angiostatin induces and sustains dormancy of human primary tumors in mice. Nat. Med. *2*, 689–692.

Overall, C.M. and Kleifeld, O. (2006). Tumour microenvironment-opinion: validating matrix metalloproteinases as drug targets and anti-targets for cancer therapy. Nat. Rev. Cancer *6*, 227–239.

Sakai, H., Saku, T., Kato, Y., and Yamamoto, K. (1989). Quantitation and immunohistochemical localization of cathepsin E and D in rat tissues and blood cells. Biochim. Biophys. Acta *991*, 367–375.

Sasaki, T., Fukai, K.M., Mann, K., Gohring, W., Olsen, B.R., and Timpl, R. (1998). Structure, function and tissue form of the C-terminal globular domain of collagen XVIII containing the angiogenesis inhibitor endostatin. EMBO J. *17*, 4249–4256.

Sastradipura, D.F., Nakanishi, H., Tsukuba, T., Nishishita, K., Sakai, H., Kato, Y., Gotow, T., Uchiyama, Y., and Yamamoto, K. (1998). Identification of cellular compartments involved in processing of cathepsin E in primary cultures of rat microglia. J. Neurochem. *70*, 2045–2056.

Sealy, L., Mota, F., Rayment, N., Tatnell, P., Kay, J., and Chain, B. (1996). Regulation of cathepsin E expression during human B cell differentiation *in vitro*. Eur. J. Immunol. *26*, 1838–1843.

Standker, L., Schrader, M., Kanse, S.M., Jurgens, M., Forssmann, W., and Preissner, K.T. (1997). Isolation and characterization of the circulating form of human endostatin. FEBS Lett. *420*, 129–133.

Strand, S., Vollmer, P., Abeelen, L., Gottfried, D., Alla, V., Heid, H., Kuball, J., Theobald, M., Galle, P.R., and Strand, D. (2004). Cleavage of CD95 by matrix metalloproteinase-7 induces apoptosis resistance in tumour cells. Oncogene *23*, 3732–3736.

Tannock, I. and Rotin, D. (1989). Acid pH in tumors and its potential for therapeutic exploitation. Cancer Res. *49*, 4373–4384.

Tominaga, K., Nakanishi, H., Yasuda, Y., and Yamamoto, K. (1998). Excitotoxin-induced neuronal death is associated with response of a unique intracellular aspartic proteinase, cathepsin E. J. Neurochem. *71*, 2574–2584.

Tsukuba, T., Okamoto, K.. Okamoto, Y., Yanagawa, M., Kohmura, K., Yasuda, Y., Uchi, H. Nakahara, T., Furue, M., Nakayama, K., et al. (2003). Association of cathepsin E deficiency with development of atopic dermatitis. J. Biochem. *134*, 893–902.

Tsukuba, T., Yamamoto, S., Yanagawa, M., Okamoto, K., Okamoto, Y., Nakayama, K.I., Kadowaki, T., and Yamamoto, K. (2006). Cathepsin E-deficient mice show increased susceptibility to bacterial infection associated with the decreased expression of multiple cell surface Toll-like receptors. J. Biochem. *140*, 57–66.

van Bokhoven, A., Varella-Garcia, M., Korch, C., Johannes, W.U., Smith, E.E., Miller, H.L., Nordeen, S.K., Miller, G.J., and Lucia, M.S. (2003). Molecular characterization of human prostate carcinoma cell lines. Prostate *57*, 205–225.

van Ravenswaay, C.H.H., Kluin, P.M., and Fleuren, G.J. (1992). Tumor infiltrating cells in human cancer. On the possible role of $CD16^+$ macrophages in antitumor cytotoxicity. Lab. Invest. *67*, 166–174.

Varney, M.L., Olsen, K.J., Mosley, R.L., Bucana, C.D., Talmadge, J.E., and Singh, R.K. (2002). Monocyte/macrophage recruitment, activation and differentiation modulate interleukin-8 production: a paracrine role of tumor-associated macrophages in tumor angiogenesis. In Vivo *16*, 471–477.

Wike-Hooley, J., Haveman, J., and Reinhold, H.S. (1984). The relevance of tumor pH in the treatment of malignant disease. Radiother. Oncol. *2*, 342–366.

Yamaguchi, N., Anand-Apte, B., Lee, M., Sasaki, T., Fukai, N., Shapiro, R., Que, I., Lowik, C., Timpl, R., and Olsen, B.R. (1999). Endostatin inhibits VEGF-induced endothelial cell migration and tumor growth independently of zinc binding. EMBO J. *18*, 4414–4423.

Yanagawa, M., Tsukuba, T., Okamoto, K., Takii, R., Terada, Y., Kadowaki, T., and Yamamoto, K. (2006). Up-regulation, enhanced maturation, and secretion of cathepsin E in mouse macrophages treated with interferon-γ or lipopolysaccharide. J. Oral Biosci. *48*, 218–225.

Yanagawa, M., Tsukuba, T., Nishioku, T., Okamoto, Y., Okamoto, K., Takii, R., Terada, Y., Nakayama, K.I., Kadowaki, T., and Yamamoto, K. (2007). Cathepsin E deficiency induces a novel form of lysosomal storage disorder showing the accumulation of lysosomal sialoglycoproteins and the elevation of lysosomal pH in macrophages. J. Biol. Chem. *282*, 1851–1862.

Yasuda, Y., Kohmura, K., Kadowaki, T., Tsukuba, T., and Yamamoto, K. (2005). A new selective substrate for cathepsin E based on the cleavage site sequence of α2-macroglobulin. Biol. Chem. *386*, 299–305.

Received June 7, 2007; accepted August 8, 2007